Modelling of a Francis Turbine Runner Fatigue Failure Process Caused by Fluid-Structure Interaction

A. Lyutov[1], A. Kryukov[1], S. Cherny[2], D. Chirkov[2], A. Salienko[3], V. Skorospelov[4] and P. Turuk[4]

[1] Novosibirsk State University, 2 Pirogova St., Novosibirsk, Russian Federation, 630090
[2] Institute of Computational Technologies SB RAS, 6 Academic Lavrentjev Ave., Novosibirsk, Russian Federation, 630090
[3] Public joint stock company Tyazhmash, 13 Hydroturbinnaya St., Syzran, Russian Federation, 446010
[4] Sobolev Institute of Mathematics SB RAS, 4 Academic Koptyuga Ave., Novosibirsk, Russian Federation, 630090

Abstract. In the present paper considered is the problem of the numerical simulation of Francis turbine runner fatigue failure caused by fluid-structure interaction. The unsteady 3D flow is modeled simultaneously in the spiral chamber, each wicket gate and runner channels and in the draft tube using the Euler equations. Based on the unsteady runner loadings at each time step stresses in the whole runner are calculated using the elastic equilibrium equations solved with boundary element method. Set of static stress-strain states provides quasi-dynamics of runner cyclic loading. It is assumed that equivalent stresses in the runner are below the critical value after which irreversible plastic processes happen in the runner material. Therefore runner is subjected to the fatigue damage caused by high-cycle fatigue, in which the loads are generally low compared with the limit stress of the material. As a consequence, the stress state around the crack front can be fully characterized by linear elastic fracture mechanics. The place of runner cracking is determined as a point with maximal amplitude of stress oscillations. Stress pulsations amplitude is used to estimate the number of cycles until the moment of fatigue failure, number of loading cycles and oscillation frequency are used to calculate runner service time. Example of the real Francis runner which has encountered premature fatigue failure as a result of incorrect durability estimation is used to verify the developed numerical model.

Keywords: Francis turbine, rotor-stator interaction, high cycle fatigue failure

1. Introduction

In the present article an example of Francis turbine with a runner fatigue crack is studied. The considered power plant has average specific speed n_q=49, the runner diameter is D_1=2.2m. The crack which has appeared after 1067 working hours and 422 launches is shown in 1. The amount of working hours at different operating regimes is shown in Fig. 2. The goal of the present paper is to develop a software tool which will be able to a priori analyze hydraulic turbine runner in order to obtain the reliable estimation of lifetime during the design process. In addition, the most dangerous operating conditions in terms of fatigue failure are revealed. It has been shown in the present paper that the best efficiency operating point is not the one of them.

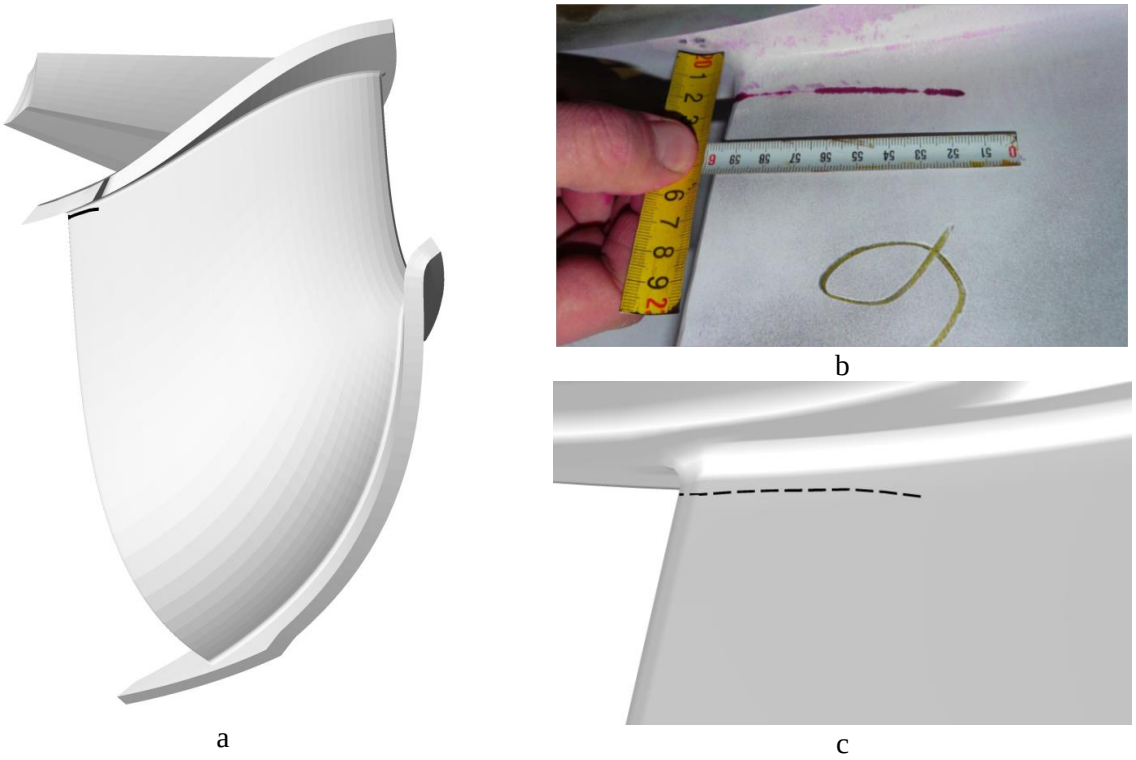

a b c

Fig. 1. Suction side of blade segment with crack (a), photograph of crack near the trailing edge at the suction side of blade(b), geometrical model of blade with displayed crack position (c).

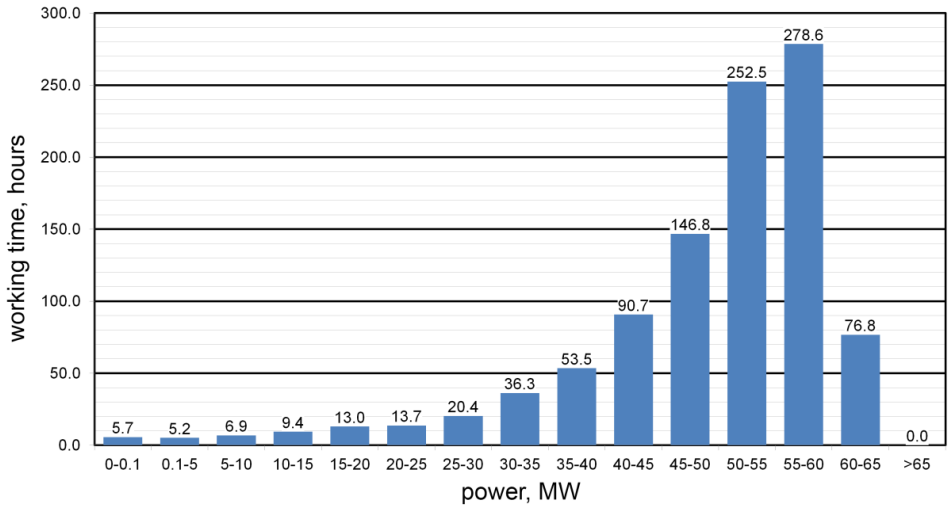

Fig. 2. Distribution of damaged hydraulic turbine working hours between the regimes.

There are more and more papers in the world concerning this problem, for example [1-11]. In [1] lifetime of runner is estimated using the dynamical stresses. Unsteady 3D incompressible fluid flow is calculated in the full statement in spiral chamber, wicket gate, runner and draft tube. Flow is described using the URANS equations with $k-\omega$ turbulence model at the low power operating point. Stress oscillations with dominating draft tube vortex rope loadings are calculated from the elastic oscillations equation

$$\rho\frac{\partial^2\bar{u}}{\partial t^2}=(\lambda+\mu)\nabla\nabla\cdot\bar{u}+\mu\Delta\bar{u}+\rho\bar{F}\,, \tag{1.1}$$

which after discretization turns into

$$\left[M_s\right]\{\ddot{u}\}+\left[C_s\right]\{\dot{u}\}+\left[K_s\right]\{u\}=\{F_s\}+\{F_t\}\,, \tag{1.2}$$

and is solved with Newmark's algorithm [2].

In [3] time of fatigue cracks appearance in a runner is calculated by a local displacements analysis [4] in equation

$$\frac{1}{2}\Delta\varepsilon=\frac{\sigma_f^{'}-\sigma_m}{E}\left(2N_i\right)^b+\varepsilon_f^{'}\left(2N_i\right)^c\,, \tag{1.3}$$

which connects the number of loading cycles until crack initiation N_i with amplitude of deformation $\Delta\varepsilon$. To do so, system of fluid-structure interaction equations is solved. System consists of equation (1.2) and Helmholtz equation

$$\Delta P=\frac{1}{c^2}\frac{\partial^2 P}{\partial t^2}\,, \tag{1.4}$$

that describes acoustic waves in fluid. After discretization of system (1.2), (1.4) using finite element method and using condition on the border between the fluid and structure $\{n\}\cdot\nabla P=-\rho_f\{n\}\cdot\frac{\partial^2 u}{\partial t^2}$ system turns into

$$\begin{pmatrix}M_s & 0\\ M_{fs} & M_f\end{pmatrix}\begin{pmatrix}\{\ddot{u}\}\\ \{\ddot{p}\}\end{pmatrix}+\begin{pmatrix}C_s & 0\\ 0 & C_f\end{pmatrix}\begin{pmatrix}\{\dot{u}\}\\ \{\dot{p}\}\end{pmatrix}+\begin{pmatrix}K_s & K_{fs}\\ 0 & K_f\end{pmatrix}\begin{pmatrix}\{u\}\\ \{p\}\end{pmatrix}=\begin{pmatrix}\{F_s\}\\ \{0\}\end{pmatrix}. \tag{1.5}$$

Natural frequencies of runner in water are found as eigenvalues of system (1.5). Static stresses are calculated with consideration of centrifugal force and static pressure. Dynamic stress amplitude comes from the static considering excitation force coefficient. Then, using the Neuber rule [5] and total strain expression

$$\frac{\left(K_f\Delta S\right)^2}{E}=\Delta\varepsilon\Delta\sigma\,,\qquad \frac{1}{2}\Delta\varepsilon=\frac{1}{2E}\Delta\sigma+\left(\frac{1}{2K^{'}}\Delta\sigma\right)^{\frac{1}{n^{'}}}\,, \tag{1.6}$$

amplitude of deformation $\Delta\varepsilon$ is calculated and put into (1.3). Afterwards, with frequency of excitation force f time estimation is obtained

$$T=\frac{N_i}{f}\,, \tag{1.7}$$

In [6] based on known dynamic stresses in a Kaplan turbine piston rod from equation (1.3), estimation of fatigue crack initiation time is obtained. Stress intensity factor in polar coordinate system (r,θ) with origin at the crack tip is calculated by formula

$$K=\frac{\sigma_{ij}(r,\theta)\sqrt{\pi a}}{f_{ij}(\theta)}\,, \tag{1.8}$$

where a is crack length. Then structure service time is estimated using the Paris-Erdogan relation [7]

$$\frac{da}{dN} = C\left(\Delta K\right)^m, \tag{1.9}$$

where mixed mode stress intensity factor range ΔK_{MM} is used instead of ΔK. Therefore, the dependence between crack length and number of loading cycles allows estimating the structure lifetime as a sum of crack initiation time and time required by the crack to reach critical length.

In [8] based on the local stress measurements relative damage factor C is calculated for five hydraulic turbine runners operating in different regimes such as part load, low part load, speed-no-load and during start-stops and load rejection. Relative damage factor shows runner fatigue capacity under effect of k different dynamical stresses with amplitude σ_i after n_i cycles. To do so, linear cumulative fatigue damage theory or Miner rule is used

$$\sum_{i=1}^{k} \frac{n_i}{N_i} = C, \tag{1.10}$$

where N_i is the number of cycles until the failure under loading σ_i. Similar approach is used in the [9] where in contrast dynamical loading are simulated numerically.

In [10, 11] the mechanisms of crack propagation in hydroturbine runner's welding joints are investigated. Crack propagation under cyclic loadings is described using the Paris-Erdogan relation (1.9).

The most of the used approaches have got several important limitations like considering slightly simplified, cyclic or static hydrodynamics, calculating in reduced computational domain without spiral chamber that does not account rotor-stator interaction, performing stress analysis for a separated blade or a runner segment. In the present paper the stated problem is solved comprehensively, considering all of those factors.

2. CFD Modelling

2.1. Domain setup and meshing

The flow in a spiral chamber, being circumferentially non-uniform, causes influence on pressure oscillations in the runner. Therefore it is required to simulate the flow in the whole spiral chamber, wicket gate and runner in order to model rotor-stator interaction precisely. To account the loadings resulting from a vortex rope domain setup should include draft tube (Fig. 3).

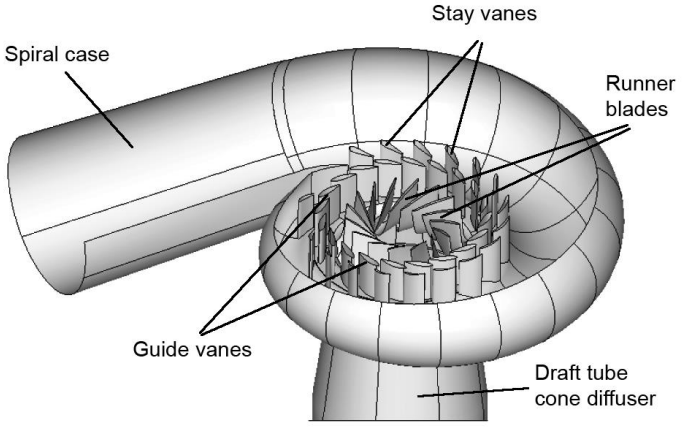

Fig. 3. Computational domain for unsteady flow simulation in the whole turbine domain.

2.2. Governing equations and numerical method

The unsteady runner loads caused by rotor-stator interaction and a vortex rope can be accurately predicted using the Euler equations [12]. In this case the system is written as:

$$\frac{\partial u_j}{\partial x_j} = 0\,, \tag{2.1}$$

$$\frac{\partial u_i}{\partial t} + \frac{\partial \left(u_i u_j\right)}{\partial x_j} + \frac{\partial p}{\partial x_i} = f_i\,,\ i = 1,2,3\,, \tag{2.2}$$

where f_i is the component of external forces vector, such as gravity, centrifugal and Coriolis forces.

The numerical method of solving this system used in the present paper is based on introducing an artificial compressibility into the continuity equation. The modified system of equations is discretized using an implicit finite-volume scheme. The fluxes are evaluated with a third-order MUSCL scheme. The resulting nonlinear system of discrete equations is linearized and approximately lower upper (LU)-factorized which enables the computation of unknowns in two sweeps of computational domain, one in the direction of increasing cell indices and another in the direction of decreasing indices. A modetailed description of the used numerical method can be found in [13, 14].

2.3. Unsteady CFD results

As it is mentioned in the introduction, turbine got damaged after 1067 hours of working and 422 turbine launches. It is also important that more than the half of working time turbine has been working on the regimes between 50 and 60 MW, which can be seen in Fig. 2. After runner restoration full-scale experiment has been performed in which turbine characteristics during start-stop, speed-no-load, part-load, and best efficiency operating conditions were gauged. Figures 4 and 5 show the value of the generator power output N during the experiment and the stress data, respectively. The stress data has been collected from a stress gauge near the crack origin. As long as best efficiency point in the experiment corresponds to the power of 50 MW, this regime is modeled in unsteady numerical simulation. It is clear that this operating point has the smallest stress amplitude in the whole experiment and can hardly be seen in the figure. Therefore, the comparison between the calculated stress and the experimental data would not be performed here. This comparison would be of an interest during the further simulations at part load and startup. However, for the purpose of a step-by-step discussion, this data is given here.

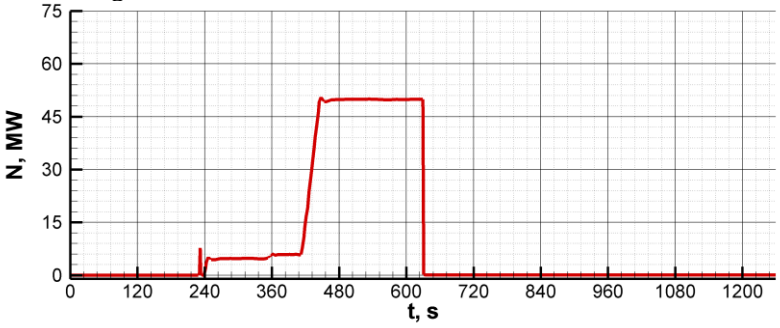

Fig. 4. Power output during the experiment.

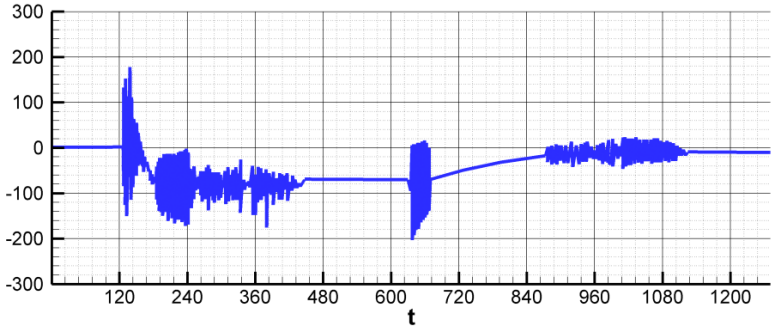

Fig. 5. Stress gauge data during the experiment.

Even though this operation point usually does not suffer from vortex rope, computational domain consisted of whole turbine flow duct including draft tube. Flow is simulated with fixed discharge that corresponds to regime with the selected power. Computational grid consists of 3.9 million nodes and is shown in Fig. 6, 7.

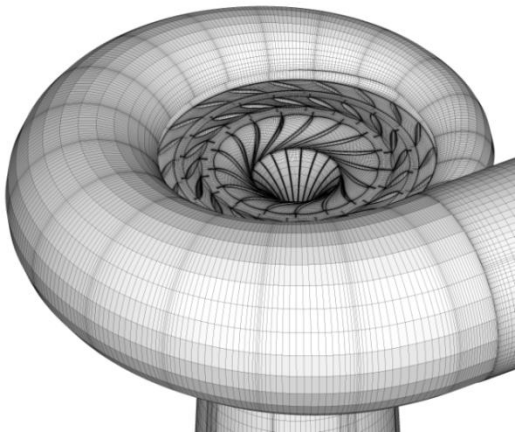

Fig. 6. Computational mesh in spiral chamber, wicket gate and runner.

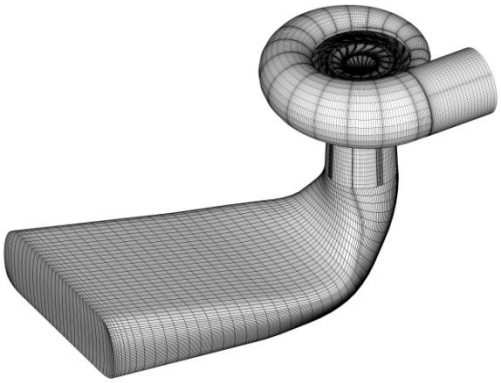

Fig. 7. Computational mesh in whole flow duct.

The pressure oscillations at a point on the leading edge (LE) and the trailing edge (TE) are shown in Fig. 8. The point at the TE is positioned near the place of the real runner crack. The positions of points and the pressure distribution on the sides of the blade at the time moment t=0.58s are shown in Fig. 9.

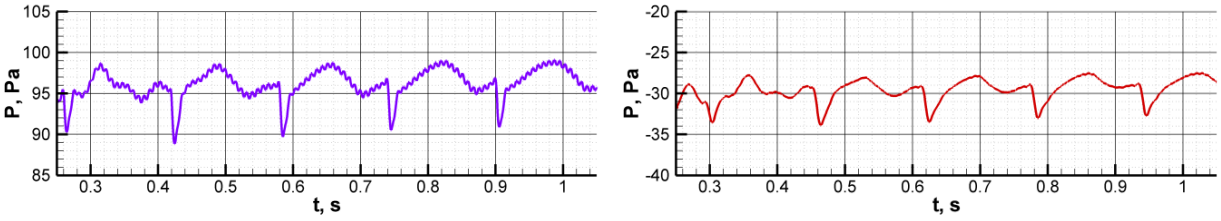

leading edge trailing edge

Fig. 8. Pressure oscillations at points on leading and trailing edges of runner.

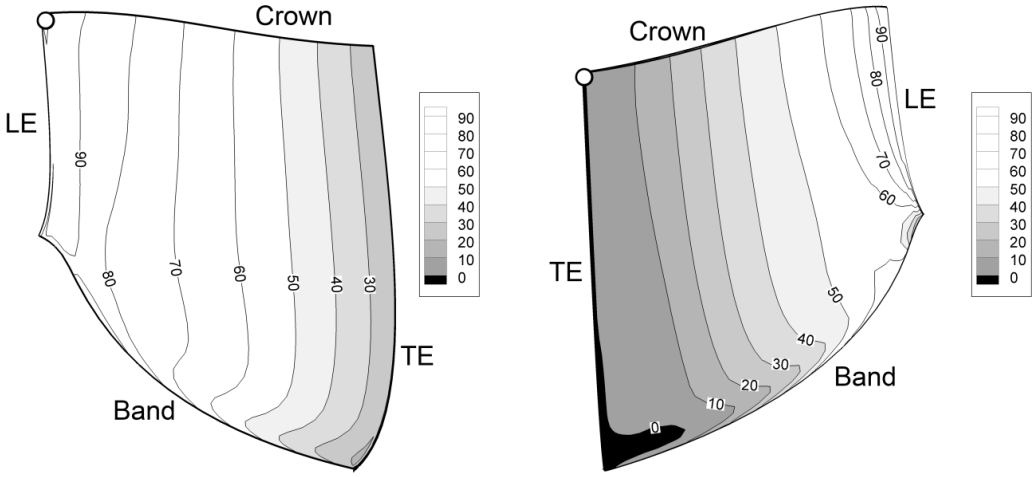

pressure side suction side

Fig. 9. Pressure distribution over the blade at t=0.58sec. Pressure for Fig. 8 is measured at the labeled points.

3. Stress modelling

3.1. Domain setup and meshing

Stress-strain state of the runner is performed for the whole runner. Part of the crown upper side is considered fixed $\bar{u}=0$ as it is fixed to the turbine shaft. At each time step hydraulic pressure p_{hydro} is defined as a boundary condition at runner flow channels. All other runner surfaces are considered traction-free, that is $p=0$ Fig. 10. As a result a quasi-dynamic evolution of stress in the runner is obtained.

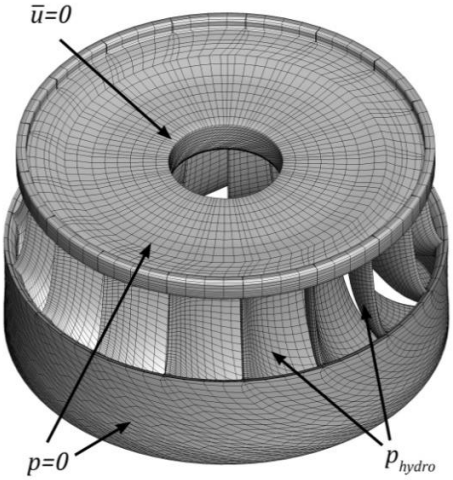

Fig. 10. Mesh and boundary conditions for stress analysis.

3.2. Governing equations and numerical method

Stress-strain state of isotropic uniform material (steel) under hydrodynamic, gravity and centrifugal forces is described by the elastic oscillations equation

$$(\lambda+\mu)\nabla\nabla\cdot\bar{u}+\mu\Delta\bar{u}+\rho\bar{b}=\rho\frac{\partial^2\bar{u}}{\partial t^2}. \tag{3.1}$$

In a quasi-dynamic approach term $\rho\frac{\partial^2\bar{u}}{\partial t^2}$ in equations (3.1) is considered to be negligible, therefore the static equilibrium equations are valid

$$(\lambda+\mu)\nabla\nabla\cdot\bar{u}+\mu\Delta\bar{u}+\rho\bar{b}=0. \tag{3.2}$$

Then, transference from the differential equation to integral

$$u_j(x)=\int_S U_{ij}(x',x)t_i(x')dS-\int_S T_{ij}(x',x)u_i(x')dS,\quad i,j=1,2,3 \tag{3.3}$$

is performed. It connects values only on the runner boundary S. After discretization of the boundary and approximation of equations (3.3) , system of linear equations

$$T\bar{u}=U\bar{t}\,. \tag{3.4}$$

is obtained. It connects components of displacements vector $\bar{u}$ and components of tensions vector $\bar{t}=\sigma n$ at the boundary points. Then $\mathbb{LU}$-factorization of matrix T is performed and using the back substitution in Gauss method components of displacements vector $\bar{u}$ are obtained.

3.3. Stress-strain simulation results

The point of possible cracking is considered the place with maximal stress amplitude. In order to estimate the position of crack, calculation of stress amplitude in each node of computational grid is performed. Peak amplitude level is observed at the border between the suction side of the blade and the trailing edge, near the crown as can be seen in Fig. 11. It should be noted that zone of maximal amplitude is situated near the point of real runner cracking. Figure 12 shows the equivalent stresses at

the same area at the moment of peak oscillation. It should be noted that the point of maximal stress coincides with the point of maximal amplitude.

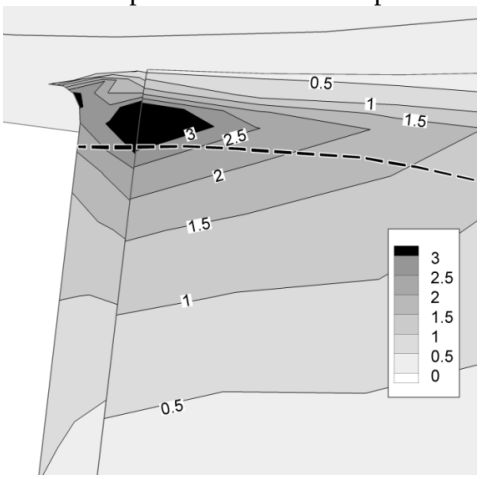

Fig. 11. Double amplitude of stress oscillations at the trailing edge near the crown.

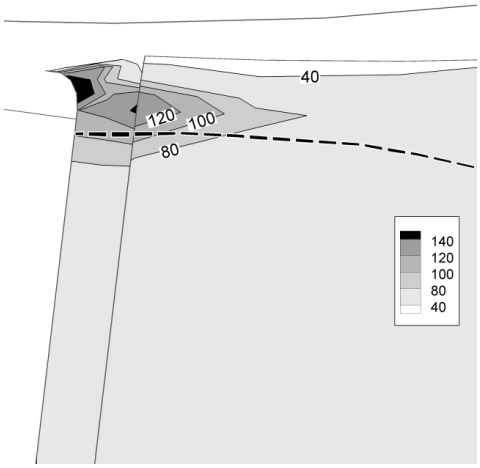

Fig. 12. Equivalent stress at the moment of peak loadings.

The oscillations of the equivalent stress at the point of maximal amplitude and their spectrum are shown in figures 13 and 14 respectively. In the spectral analysis there are distinct stress pulsations with rotational frequency f_n, and wicket gate frequency $f_{WG} = n_{WG} f_n$. Also there are doubled and trebled rotational frequencies, which might be a result of analysis noise but also will be considered for the fatigue analysis.

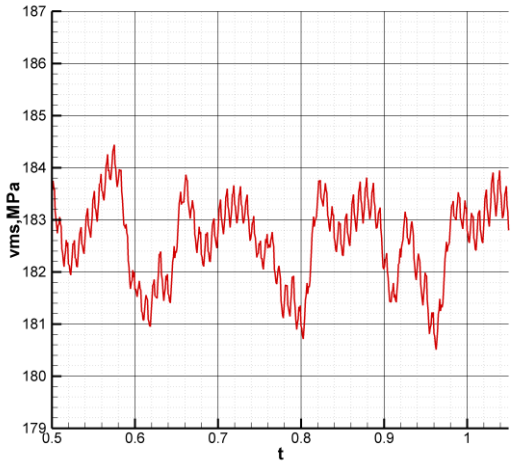

Fig. 13. Equivalent stress oscillations at the peak amplitude point.

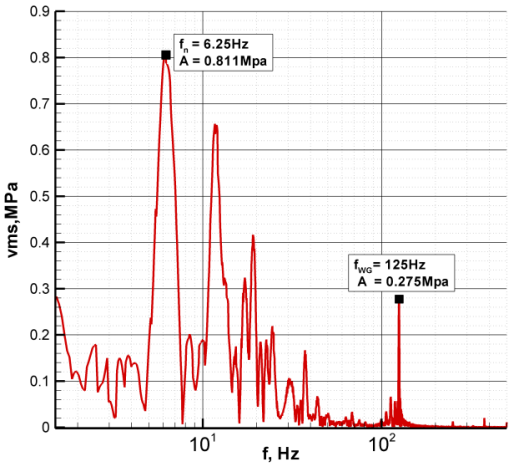

Fig. 14. Spectrum of stress oscillations.

4. Fatigue life assessment

4.1. General considerations

The main factors that influence structure fatigue life under dynamic loadings are the alternating stress amplitude σ_a, mean stress σ_m, material parameters and structure sizes. Mean stress consists of static and residual stresses $\sigma_m = \sigma_s + \sigma_0$. If the static stress and alternating stress amplitude are defined by the external forces that influence the structure, the residual stress also known as technological are appearing during the manufacturing processes.

The turbine runner considered in the present paper was manufactured from steel grade GX4CrNiMo13-4. Its yield strength is estimated by 600 MPa. In accordance to the article [15],

residual stress lie in the range between 10% and 25% of the yield strength, that is 60 to 150 MPa for the above mentioned steel. Peak stress in the runner from the stress simulation are 184.5 Mpa. Therefore, in the worst case the overall stress in the runner equals 334.5MPa, that is almost two time lower than the yield strength. This means that deformations in the runner under these operating conditions are elastic and estimation of the runner fatigue lifetime should be performed using the SN approach. The following formula provides us with correlation between the alternating stress amplitude σ_a and number of loading cycles N with such amplitude until the moment of fatigue failure

$$\lg\sigma_a = A + B\lg N, \tag{4.1}$$

where coefficients A and B depend on the material properties and runner dimensions and are estimated experimentally for the specimens of different sizes. For the runner considered in the present paper the following coefficients have been taken: A=2.6606, B=-0.0791.

4.2. Cumulative fatigue

During the turbine service even in a single operating point runner is subjected to the whole spectrum of stress oscillations with different frequencies and amplitudes. It is commonly believed [9] that cumulative damage from the different stress oscillations can be linearly summarized.

Let us assume that during the turbine operates on a steady regime and runner is affected by k different simple stress oscillations, each of which will separately lead to fatigue failure after N_i cycles or after time,

$$t_i = N_i / f_i, \tag{4.2}$$

where f_i is the frequency of corresponding pulsation. After time t each oscillation produces $f_i t$ cycles to the runner and when this number becomes greater or equal to N_i, it means that fatigue failure happens. This can be rewritten as

$$\frac{f_i t}{N_i} = C, \tag{4.3}$$

where C is the amount of damage the runner has received from stress oscillation i after time t, $C \geq 1$ is fatigue failure. When several oscillations affect runner simultaneously, total damage they cause after time t is

$$\left(\sum_{i=1}^{k} \frac{f_i}{N_i}\right) t = C. \tag{4.4}$$

From equation (4.4) using the (4.2) cumulative fatigue failure time can be obtained:

$$t = \left(\sum_{i=1}^{k} \frac{1}{t_i}\right)^{-1}. \tag{4.5}$$

From the stress calculation in section 3, it can be seen that runner is affected by a pulsation with rotational frequency f_n =6.25 Hz and a pulsation with wicket gate frequency f_{WG} =125 Hz. Other noticeable pulsations are doubled and trebled rotational frequencies. Time of fatigue life for each pulsation resulting from equation (4.1) is provided in the table 1.

Table 1. Fatigue lifetime for simple stress oscillations.

	f, Hz	N_i, cycles	t_i, years
f_n	6.18	6.1E+34	3.1E+26
$2f_n$	11.9	9.2E+35	2.5E+27
$3f_n$	19.1	2.8E+38	4.6E+29
f_{WG}	125	5.4E+40	1.4E+31

The cumulative fatigue failure lifetime calculated from the equation (4.5) is $t = 2.8 \cdot 10^{26}$ years, which is many times the amount required during the design process.

5. Conclusions

Based on the developed methodology an estimation of runner fatigue lifetime during the operation in the best efficiency operating point has been performed. Results show that the fatigue failure happened to the real runner could not have been induced by the loading on the regime, where turbine has been operating most of the time. In accordance to the operational data there were numerous starts and stops during the service time. Such transient regimes are considered very dangerous and damaging for the runner.

6. Acknowledgements

This work was supported by grant №14-01-00278 of Russian Foundation for Basic Research.

7. References

[1] Ruofu X, Zhengwei W and Yongyao L 2008 Dynamic Stresses in a Francis Turbine Runner Based on Fluid-Structure Interaction Analysis // *Tsinghua Science and Technology*, **13**, 587-592.

[2] Newmark N M 1959 A method of computation for structural dynamics // *Journal of Engineering Mechanics*, ASCE, pp. 67-94.

[3] Flores M, Urquiza G and Rodríguez J 2012 A Fatigue Analysis of a Hydraulic Francis Turbine Runner // *World Journal of Mechanics*, **2**, No. 1, pp. 28-34

[4] Martin J F, Topper T H and Sinclair G M 1969 Computer based simulation of cyclic stress strain behavior // *T.&A.* M. Report No. 326, University of Illinois, Urbana

[5] Huth H J 2005 Fatigue Design of Hydraulic Turbine Runners // *PhD Thesis, Norwegian University of Science and Technology*

[6] Liu X., Luo Y.Y. and Wang, Z.W., 2014, Fatigue Analysis of the Piston Rod in a Kaplan Turbine Based on Crack Propagation under Unsteady Hydraulic Loads // *IOP Conference Series: Earth and Environmental Science*

[7] Paris A and Erdogan F 1963 A critical analysis of crack propagation law // *J. Basic Eng.*, **85**, pp. 528–534

[8] Huang X, Chamberland-Lauzon J, Oram C, Klopfer A. and Ruchonnet N 2014 Fatigue analyses of the prototype Francis runners based on site measurements and simulations // *IOP Conference Series: Earth and Environmental Science*, **22**

[9] Magnoli M V 2014 Numerical simulation of pressure oscillation in large Francis turbines at partial and full load operating conditions and their effects // *Ph.D. thesis, Technische Universität München*

[10] Trudel A and Sabourin M 2014 Metallurgical and fatigue assessments of welds in cast welded hydraulic turbine runners // *IOP Conference Series: Earth and Environmental Science*, **22**

[11] Carpinteri A, Ronchei C, Scorza D and Vantadori S 2015 Fracture mechanics based approach to fatigue analysis of welded joints // *Engineering Failure Analysis*, **49**, pp. 67–78

[12] Yeshkunova I, Cherny S and Chirkov D 2011 Acceleration of solution convergence for the unsteady fluid problems // *Computational Technologies*, **16(5)**, pp.30-49 (In Russian)

[13] Cherny S, Chirkov D, Lapin V, Lobareva I, Sharov S and Skorospelov V 2005 3D Euler Flow Simulation in Hydro Turbines: Unsteady Analysis and Automatic Design // *Notes on Numerical Fluid Mechanics and Multidisciplinary Design*, **93**, Springer, pp. 33–51

[14] Cherny S, Sharov S, Skorospelov V and Turuk P 2003 Methods for Three-Dimensional Flows Computation in Hydraulic Turbines, // *Russ. J. Num. Anal. Math. Model.*, **18(2)**, pp. 87–104.

[15] Sabourin M, Thibault D, Bouffard D and Lévesque M 2010 New parameters influencing hydraulic runner life time // *IOP Conference Series Earth and Environmental Science*, 12(1):012050, pp. 1-9.